Archives of Hydro-Engineering and Environmental Mechanics
Vol. 51 (2004), No. 3, pp. 287–303

Implicit versus Explicit Finite Volume Schemes for Extreme, Free Surface Water Flow Modelling

Michał Szydłowski

Gdańsk University of Technology, Faculty of Hydro- and Environmental Engineering,
ul. Narutowicza 11/12, 80-952 Gdańsk, e-mail: mszyd@pg.gda.pl

(Received April 22, 2004; revised July 05, 2004)

Abstract

One explicit and three implicit finite volume method schemes of the Roe type are presented in the paper. The properties and applicability of these methods for modelling unsteady, rapidly varied, open channel flow are investigated. The schemes are used for numerical simulation of one-dimensional extreme flow described by de Saint-Venant equations. The computational results are compared with each other and an analytical (exact) solution to an idealized dam-break problem. The classical versions of general scheme implicit in time – fully implicit and trapezoidal scheme – are not restricted by a stability condition, like an explicit one, however they add some numerical diffusion and dispersion errors to the solution. The modification of parameter Θ, originally proposed for a box scheme of finite difference method, has improved computational properties of the general one-step implicit scheme. This version of finite volume scheme of the Roe type implicit in time can be recommended for modelling and simulation of transient flows in storm sewers and open channel networks.

Key words: general scheme implicit in time, finite volume method, extreme flows

1. Introduction

In recent years considerable effort has been devoted to modelling one- and two-dimensional open channel flows. The free surface one-dimensional, unsteady water flow is governed by the well-known mathematical model called de Saint-Venant equations (Abbott 1979). Quite a number of numerical methods of solving this equations system have been proposed and successfully applied, so far. For the gradually varied flow simulation numerous schemes of finite difference method (FDM) and finite element method (FEM) are widely used (Cunge et al 1980, Szymkiewicz 2000). Unfortunately, the FDM and FEM numerical procedures are often inefficient for modelling rapidly varied, transient flow, when discontinuities such as hydraulic jumps and bores exist.

For this kind of flow, shock-capturing methods must be implemented to solve the conservative form of de Saint-Venant equations (Abbott 1979). Many of these methods are based on the finite volume method (FVM) applied for space discretization. To model the free surface flow, the FVM schemes of the Roe type, originally developed for gas dynamics (Roe 1981), are widely used (Glaister 1993, Ambrosi 1995, Toro 1997, Szydłowski 2001, Goutal and Maurel 2002).

In shock-capturing methods, schemes explicit rather than implicit in time are usually used. Hence, there are numerous analyse of FVM explicit schemes available in the literature (Delis et al 2000a, Zoppou and Roberts 2003). These schemes are reported as efficient and robust, but are conditionally stable. The stability of explicit schemes for hyperbolic equations is restricted by the well known Courant-Fredrichs-Lewy (CFL) condition (Potter 1977) and limited to Courant number less than unity. To avoid this disadvantage, implicit schemes can be used for time integration. However, investigations and applications of such schemes for rapidly varied water flow are rather unique (Alcrudo et al 1994, Delis et al 2000b).

This paper focuses on the FVM Roe one-step scheme implicit in time. It is examined against a two-step explicit scheme applied for numerical solution to one-dimensional open channel, extreme flow. Application of the implicit integration technique for de Saint-Venant equations results in the system of non-linear, algebraic equations. To solve such system, either an iterative procedure or less computational time consuming linearization process at each time level is required. Here, following Alcrudo et al (1994), the latter technique is implemented.

In order to assess the applicability and numerical features of particular schemes they were implemented to simulate the extreme, rapidly varied flow occurring in horizontal and frictionless open channel due to sudden, catastrophic dam collapse.

2. Governing Equations and Finite Volume Space Discretization

The unsteady one-dimensional open channel flow can be described by de Saint-Venant equations, originally proposed by French researcher in 1871 as a flood wave propagation model in the following form (Szymkiewicz 2000):

$$\frac{\partial h}{\partial t} + \frac{\partial}{\partial x}(uh) = 0, \tag{1a}$$

$$\frac{\partial u}{\partial t} + u\frac{\partial u}{\partial x} + g\frac{\partial h}{\partial x} = g\left(S_0 - S_f\right), \tag{1b}$$

where u is the flow mean velocity, h water depth, g acceleration due to gravity, x and t represent distance and time, and S_0 and S_f denote bed and friction slopes, respectively. The friction slope can be defined by Manning's formula, which for the rectangular channel of unit width has the form:

$$S_f = \frac{n^2 u\,|u|}{h^{4/3}}. \tag{2}$$

The mathematical model (Eqs. 1a, b) describes properly gradually varied, one-dimensional free surface flow. Unfortunately, this non-conservative form of equations is inconvenient for rapidly varied flow, where solution discontinuities are expected. It was proved (Abbott 1979) that the water flow with discontinuities can be described by the conservative form of de Saint-Venant model only. This can be written in vector form as follows (Cunge et al 1980):

$$\frac{\partial \mathbf{U}}{\partial t} + \frac{\partial \mathbf{F}}{\partial x} + \mathbf{S} = 0, \tag{3}$$

where

$$\mathbf{U} = \begin{pmatrix} h \\ uh \end{pmatrix}, \quad \mathbf{F} = \begin{pmatrix} uh \\ \dfrac{(uh)^2}{h} + 0.5g\,h^2 \end{pmatrix}, \quad \mathbf{S} = \begin{pmatrix} 0 \\ -gh\left(S_0 - S_f\right) \end{pmatrix}. \tag{4a, b, c}$$

The homogenous part of equation (3) is of a hyperbolic type and is responsible for most numerical difficulties in the solution to the de Saint-Venant model for rapidly varied flow. In this paper only this part – fundamental for numerical solution to the problem – is analysed. However, it should be noted that numerical integration of source terms (Eq. 4c) must also be carried out with great attention, for flow over abrupt bathymetry and flow of small depth and large velocity (Bermudez and Vazquez 1994, Nujic 1995, Szydłowski 2001, Goutal and Maurel 2002).

Neglecting the source terms vector **S**, equation (3) can be rewritten in equivalent form as

$$\frac{\partial \mathbf{U}}{\partial t} + \mathrm{div}\mathbf{F} = 0. \tag{5}$$

To integrate the equations system (5) in space by FVM the one-dimensional domain x should be discretized into a set of N line segment cells (Fig. 1). Each cell i of length Δx_i is defined by its centre point x_i and each flow variable is averaged and constant inside the cell.

Integration of equation (5) yields for each cell i

$$\frac{\partial \mathbf{U}_i}{\partial t}\Delta x_i + \oint_{B_i} (\mathbf{Fn})\, dB = 0, \tag{6}$$

where Δx_i is the length of cell i and B_i represents the cell boundary. The first term of equation (6) represents time evolution of variables h and u inside the cell

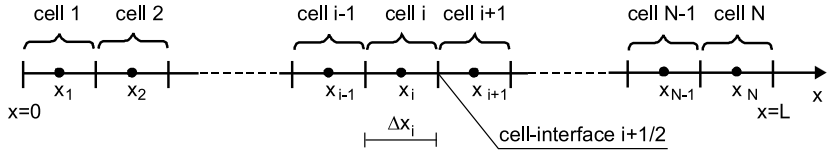

Fig. 1. Discretization of one–dimensional calculation domain

i. The surface integral represents the total normal flux through the boundary of the cell. The integral in equation (6) can be substituted by the corresponding sum of two components as follows

$$\frac{\partial \mathbf{U}_i}{\partial t}\Delta x_i + \left(\mathbf{F}_{i+1/2} - \mathbf{F}_{i-1/2}\right) = 0. \tag{7}$$

The fluxes **F** must be estimated at cell interfaces (at the boundaries between two neighbouring cells). Moreover, in order to solve equation (7) the numerical scheme should be completed with the time integration technique.

3. The Flux Computation Algorithm

In order to calculate the flux $\mathbf{F}_{i+1/2}$ the solution to approximate the Riemann problem (Godunov 1959) proposed by Roe (1981) can be applied. The full computation procedure is available in the literature (Roe 1981, Toro 1997), hence in this paper, only some significant details of the solution of de Saint-Venant equations are presented.

The original problem (Eq. 3) – neglecting the source term – can be transformed to the following form

$$\frac{\partial \mathbf{U}}{\partial t} + \mathbf{A}\frac{\partial \mathbf{U}}{\partial x} = 0, \tag{8}$$

where **U** is the same as in equation (3) and jacobian matrix $\mathbf{A}=\partial\mathbf{F}/\partial\mathbf{U}$ can be written as

$$\mathbf{A} = \begin{bmatrix} 0 & 1 \\ c^2 - u^2 & 2u \end{bmatrix}, \tag{9}$$

where $c = \sqrt{gh}$ is a celerity.

In the approximate Roe solution to the Riemann problem, the equation system (8) is linearized by replacing the jacobian **A** by averaged matrix $\overline{\mathbf{A}}$. Both forms of the jacobian matrix must be diagonalizable in the Roe approach. The above condition means that the following equation must be satisfied

$$\mathbf{A} = \mathbf{R}\,\mathbf{\Lambda}\,\mathbf{L}, \tag{10}$$

where $\mathbf{\Lambda}$ is a diagonal matrix containing the eigenvalues of matrix **A,** whereas **R** and **L** contain associated right and left eigenvectors. The eigenvalues λ_i of matrix **A** can be evaluated by solution to characteristic equation (Coulson and Jeffrey 1982)

$$|\mathbf{A} - \lambda \mathbf{I}| = 0, \tag{11}$$

where **I** is the identity matrix. Considering jacobian matrix (Eq. 9) the roots of equation (11) are equal

$$\lambda_1 = u - c, \tag{12a}$$

$$\lambda_2 = u + c. \tag{12b}$$

The corresponding right (**r**) and left (**l**) eigenvectors can be calculated solving the following equations (Coulson and Jeffrey 1982)

$$\mathbf{A}\mathbf{r}_i = \lambda_i \mathbf{r}_i \quad (i = 1, 2), \tag{13a}$$

$$\mathbf{l}_i \mathbf{A} = \lambda_i \mathbf{l}_i \quad (i = 1, 2). \tag{13b}$$

The solution to equations (13a, b) for de Saint-Venant model yields after normalization following right and left eigenvectors, respectively

$$\mathbf{r}_1 = \begin{pmatrix} 1 \\ u - c \end{pmatrix}, \qquad \mathbf{r}_2 = \begin{pmatrix} 1 \\ u + c \end{pmatrix}, \tag{14a, b}$$

$$\mathbf{l}_1 = \frac{1}{2c} \begin{pmatrix} u + c \\ -1 \end{pmatrix}, \qquad \mathbf{l}_2 = \frac{1}{2c} \begin{pmatrix} c - u \\ 1 \end{pmatrix}. \tag{15a, b}$$

Applying the Roe idea of the approximate Riemann problem solution, the numerical flux **F** at $i+1/2$ cell-interface can be expressed as

$$\mathbf{F}_{i+1/2} = 0.5\,(\mathbf{F}_L + \mathbf{F}_R) - 0.5\left|\overline{\mathbf{A}}\right|\Delta\mathbf{U}, \tag{16}$$

where subscripts L and R denote the left and right sides of $i+1/2$ cell interface, $\left|\overline{\mathbf{A}}\right|$ contains modules of matrix $\overline{\mathbf{A}}$ elements and $\Delta\mathbf{U}$ is an increment of depth and discharge between cells i and $i+1$. Alternatively, the flux (Eq. 16) can be written in equivalent form as

$$\mathbf{F}_{i+1/2} = 0.5\,(\mathbf{F}_L + \mathbf{F}_R) - 0.5\sum_{k=1}^{2} \overline{\alpha}_k \left|\overline{\lambda}_k\right| \overline{\mathbf{r}}_k, \tag{17}$$

where $\overline{\lambda}_k$ and $\overline{\mathbf{r}}_k$ are the eigenvalues and right eigenvectors of jacobian $\overline{\mathbf{A}}$, respectively. For de Saint-Venant equations the coefficients $\overline{\alpha}_k$ ($k = 1, 2$) are equal to

$$\overline{\alpha}_1 = \frac{\Delta h\,(\overline{u} + \overline{c}) - \Delta(uh)}{2\overline{c}}, \tag{18a}$$

$$\overline{\alpha}_2 = \frac{-\Delta h\,(\overline{u} - \overline{c}) + \Delta(uh)}{2\overline{c}}. \tag{18b}$$

Following the Roe (1981) proposal, the values of depth $\overline{h}$ and velocity $\overline{u}$ – needed to calculate the flux (Eq. 16 or 17) – can be evaluated as follows

$$\overline{h} = \frac{h_L + h_R}{2} \Rightarrow \overline{c} = \sqrt{g\overline{h}}, \tag{19a}$$

$$\overline{u} = \frac{\sqrt{h_L}\,u_L + \sqrt{h_R}\,u_R}{\sqrt{h_L} + \sqrt{h_R}}. \tag{19b}$$

Considering the form of Roe numerical flux (Eq. 16 or 17) it can be seen that it consists of two elements. First is an arithmetic average of fluxes computed on both sides of the cell interface and the second is part of the up-wind type.

If the conserved variables $\mathbf{U}_L$ and $\mathbf{U}_R$, necessary to estimate flux (Eq. 16 or 17), are equal to cell-centre parameters $\mathbf{U}_i$ and $\mathbf{U}_{i+1}$, respectively, then the numerical scheme is of first-order accuracy in space. In order to ensure an approximation of second-order accuracy, a function extrapolation technique can be imposed. In the schemes presented here, the function values are extrapolated from the cell centre-point to the cell interface using the reconstruction technique called the **M**onotonic **U**pstream-centred **S**cheme for **C**onservation **L**aw (MUSCL) (Van Leer 1979, Tan 1992). Applying this approach for the reconstruction of function $\mathbf{U}$, the values of flow parameters at the cell-interface $i+1/2$ can be calculated as follows

$$\begin{aligned} \mathbf{U}_L &= \mathbf{U}_i + \frac{\alpha}{4}[(1-\beta)\,(\mathbf{U}_i - \mathbf{U}_{i-1}) + (1+\beta)\,(\mathbf{U}_{i+1} - \mathbf{U}_i)], \\ \mathbf{U}_R &= \mathbf{U}_{i+1} - \frac{\alpha}{4}[(1+\beta)\,(\mathbf{U}_{i+1} - \mathbf{U}_i) + (1-\beta)\,(\mathbf{U}_{i+2} - \mathbf{U}_{i+1})]. \end{aligned} \tag{20}$$

In order to chose the type of extrapolation one can use parameters α and β. Parameter α switches the scheme from first-order accuracy ($\alpha = 0$) to second-order accuracy ($\alpha = 1$) in space. Parameter β classifies the numerical scheme as central ($\beta = 1$), up-wind ($\beta = -1$) or up-wind-biased ($\beta = 0$ or $\beta = 1/3$). To ensure good quality of solution to most practical cases Tan (1992) suggests to use $\beta = 1/3$. Hence, this value was accepted for each simulation presented in this paper.

The extrapolation (Eq. 20) creates some computational difficulties near the discontinuity regions. The spurious oscillations can appear in the solution, so

a correction of reconstruction is needed. This may be done through the application of a limiter to the reconstruction scheme (Eq. 20). The extrapolation can be limited by the parameter α. This parameter may have the form of non-linear function called limit function. Numerous forms of this function can be found in the literature (Tan 1992). Herein, the van Albada limit function was implemented:

$$\alpha = \frac{2\ \Delta\mathbf{U}^{-}\Delta\mathbf{U}^{+} + \delta}{(\Delta\mathbf{U}^{-})^2 + (\Delta\mathbf{U}^{+})^2 + \delta}, \tag{21}$$

where $\Delta\mathbf{U}^{-} = \mathbf{U}_i - \mathbf{U}_{i-1}$, $\Delta\mathbf{U}^{+} = \mathbf{U}_{i+1} - \mathbf{U}_i$ and δ is a small parameter to prevent division by zero.

4. Time Integration Technique

In order to complete the solution of equation (7) a numerical scheme of time integration must be implemented. For a computational cell i, Equation (7) can be written in another vector form

$$\frac{\partial\ \mathbf{U}_i}{\partial\ t} = \mathbf{X}_i, \tag{22}$$

where vector $\mathbf{X}$ – containing all the terms of equation (7), except for the time derivatives – can be expressed as

$$\mathbf{X}_i = -\frac{\left(\mathbf{F}_{i+1/2} - \mathbf{F}_{i-1/2}\right)}{\Delta x_i}. \tag{23}$$

The solution of equation (22) can be obtained by integration in the time increment $\langle t,\ t+\Delta t\rangle$. The general integration in time scheme – defining a new function values – can be written as follows

$$\mathbf{U}_i^{n+1} = \mathbf{U}_i^{n} + \int_{t}^{t+\Delta t} \mathbf{X}_i\, dt, \tag{24}$$

where superscripts n and $n+1$ denote previous and next time level on the numerical grid. In a discrete form it can be rewritten as one-step formula with parameter Θ

$$\mathbf{U}_i^{n+1} = \mathbf{U}_i^{n} + \Delta t\ \left(\Theta\mathbf{X}_i^{n+1} + (1-\Theta)\,\mathbf{X}_i^{n}\right). \tag{25}$$

Scheme (Eq. 25) can be realized in an explicit or implicit way. In the present work four schemes are compared – three implicit: for $\Theta = 1$ (fully implicit of first-order accuracy in time), $\Theta = 0.5$ (trapezoidal of second-order accuracy in time) and for $\Theta = 0.67$ and one explicit scheme for $\Theta = 0$. The latter, in two-step version, can be written as:

$$\mathbf{U}_i^p = \mathbf{U}_i^n + 0.5\Delta t\,\mathbf{X}_i^n, \tag{26a}$$

$$\mathbf{U}_i^{n+1} = \mathbf{U}_i^n + \Delta t\,\mathbf{X}_i^p. \tag{26b}$$

This scheme is of second-order accuracy in time, but its stability is restricted by the local value of the Courant number (Potter 1977)

$$\mathrm{Cr} = \frac{|u_i| + c}{\Delta\, x_i/\Delta t} \leq 1, \tag{27}$$

where subscript i concerns the cell. To avoid this restriction, the implicit in time scheme should be used, but for non-linear problems, such as de Saint-Venant equations, the resulting, system of algebraic equations after space and time integration is also non-linear. In order to find a solution, the use of an iterative procedure is usually required, like the Newton method for example. Such numerical technique is computationally rather expensive. To reduce the 'costs' of this time consuming process the system of equations (25) can be linearized.

The system (Eq. 25) can be rewritten as:

$$\mathbf{U}_i^{n+1} + \frac{\Delta t}{\Delta x}\,\Theta\left(\mathbf{F}_{i+1/2}^{n+1} - \mathbf{F}_{i-1/2}^{n+1}\right) = \mathbf{U}_i^n - \frac{\Delta t}{\Delta x}\,(1-\Theta)\left(\mathbf{F}_{i+1/2}^{n} - \mathbf{F}_{i-1/2}^{n}\right). \tag{28}$$

Following the same procedure as Alcrudo et al (1994) or Delis et al (2000b), the implicit part of numerical flux $\mathbf{F}^{n+1}$ in equation (28) is linearized using the Taylor expansion:

$$\mathbf{F}_i^{n+1} = \mathbf{F}_i^n + \mathbf{A}_i^n\,\delta\mathbf{U}_i + \mathrm{O}\left(\Delta t^2\right), \tag{29}$$

where $\delta\mathbf{U}_i = \mathbf{U}_i^{n+1} - \mathbf{U}_i^n$. The expansion (Eq. 29) ensures the conservative discretization consistent with Roe procedure for solving an approximate Riemann problem. Moreover, the following approximation is made:

$$\overline{\mathbf{A}}_{i+1/2}^{n+1} = \overline{\mathbf{A}}_{i+1/2}^{n}. \tag{30}$$

The introduction of simplifications (Eqs. 29, 30) and formula (16) into equation (28) yields system:

$$\mathbf{B}_1\,\delta\mathbf{U}_{i-1} + \mathbf{B}_2\,\delta\mathbf{U}_i + \mathbf{B}_3\,\delta\mathbf{U}_{i+1} = \mathbf{B}_4, \qquad i = 2,\ ...,\ N-1, \tag{31}$$

where $\mathbf{B}$ coefficients are 2×2 matrices with elements:

$$\mathbf{B}_1 = -0.5\ \Theta\ \frac{\Delta t}{\Delta x}\left(\mathbf{A}_{i-1}^n + \overline{\mathbf{A}}_{i-1/2}^n\right), \tag{32a}$$

$$\mathbf{B}_2 = \mathbf{I} + 0.5\ \Theta\ \frac{\Delta t}{\Delta x}\left(\overline{\mathbf{A}}^n_{i-1/2} + \overline{\mathbf{A}}^n_{i+1/2}\right), \tag{32b}$$

$$\mathbf{B}_3 = 0.5\ \Theta\ \frac{\Delta t}{\Delta x}\left(\mathbf{A}^n_{i+1} - \overline{\mathbf{A}}^n_{i+1/2}\right), \tag{32c}$$

$$\mathbf{B}_4 = -\frac{\Delta t}{\Delta x}\left(\mathbf{F}^n_{i+1/2} - \mathbf{F}^n_{i-1/2}\right). \tag{32d}$$

For a single channel, the equations (31) form a block, tri-diagonal system, which must be completed by a consistent set of boundary conditions. The boundary and initial conditions are not substantial for the properties of any numerical scheme, so this problem is omitted in this paper. It should be noted however, that the conditions must be imposed in accordance with the characteristics theory (Szymkiewicz 2000) and idea of FVM (Szydłowski 2001). Then, the system has to be solved at each time level. This can be done using any method for linear systems solution.

5. Numerical Computations and Results Discussion

The main interest here is to test several numerical schemes for modelling rapidly varied, extreme open channel flow. To assess the quality of a numerical solution to de Saint-Venant equation – produced with one explicit and three implicit schemes – an idealized dam-break problem is chosen as a test-case. The results for each approach are compared with an analytical (exact) solution proposed by Stoker (1957).

In the test-cases one-dimensional flow in rectangular, 1 m wide and 400 m long, frictionless channel with flat bottom is considered. Initially, two different water levels are separated from each other by a 'dam' in the middle of the channel. Before dam-break, a water body is at rest and water levels are equal to 6 and 1 m upstream and downstream, respectively. After sudden water release, two waves can be observed – shock wave travelling downstream and depression wave moving upstream. It is assumed that during simulation the waves do not reach the computational domain boundaries (channel inflow and outflow).

Each numerical simulation – presented in this paper – was carried out using a mesh composed of 800 computational cells ($\Delta x = 0.5$ m). The properties of numerical schemes were investigated for different maximum local Courant numbers varying from 0.2 to 4.5. Time integration was done using a two-step explicit in time scheme and general implicit scheme for parameter Θ equal to 1.0, 0.5 and additionally 0.67. The latter value has been proposed by Cunge et al (1980) as the optimal one for the FDM box scheme. The comparison between results obtained using various schemes for different numerical parameters is presented in Figures from 2 to 7.

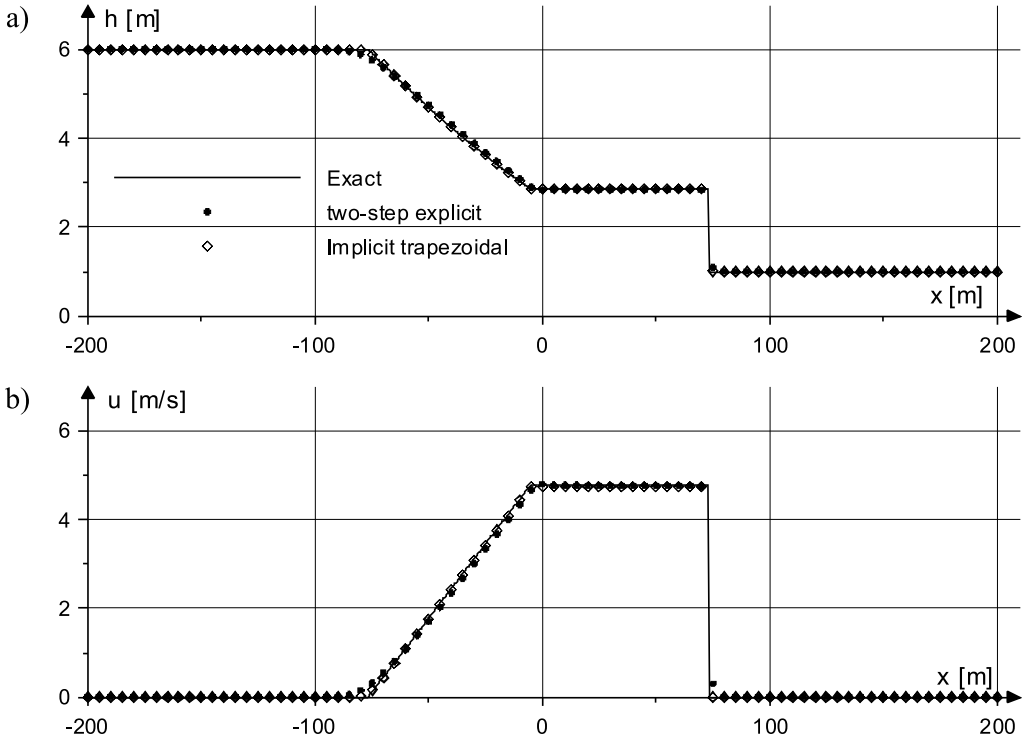

Fig. 2. Computed profiles of water depth (a) and velocity (b) after 10 s of simulation

In Figure 2 the problem solution along the channel after 10 s of simulation is presented. The numerical computations were carried out for Cr = 0.2 using the schemes of second-order accuracy in space. It required that the MUSCL technique for function reconstruction was applied. The two schemes of second-order accuracy in time – two-step explicit and trapezoidal implicit ($\Theta = 0.5$) – produced almost identical depth and velocity profiles for an assumed small Courant number. The flow parameters and front positions are correct. Some numerical diffusion can be observed near the front of the depression wave. However, the quality of numerical solution in this region depends strongly on the scheme accuracy in space, which can be seen in Figure 3.

In this graph the part of depth profile near the front of a depression wave is presented. For any time integration method, if FVM Roe scheme of first-order accuracy in space is used, the wave front is broader than for second-order accuracy. This spurious effect exists due to numerical diffusion added to the solution by dissipative first-order schemes. It should be underlined that despite different accuracy, the solution is reasonable and close to the exact one in this region and it correctly predicts location and velocity of moving wave fronts.

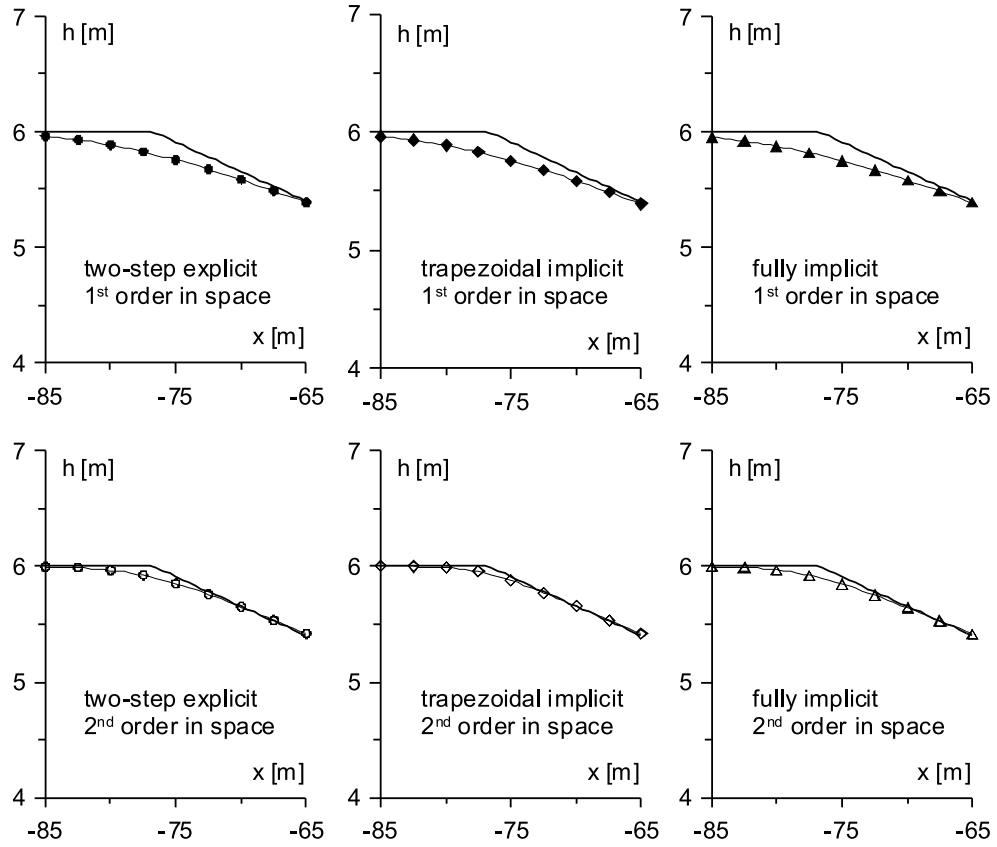

Fig. 3. Front of depression wave after 10 s of simulation – comparison between exact solution (solid lines) and computed using different schemes (symbols)

The good results' fitting decreases for a Courant number greater than about 0.8, especially when second-order in time scheme is used. The schemes' limits can be clearly observed analysing the shock wave (bore) front. The comparison of depth profile near this front, for different schemes accuracy and Courant numbers, are shown in Figures 4, 5, 6 and 7.

First, the results calculated using the explicit scheme are presented (Fig. 4a–e). For first-order in space schemes the front wave is reproduced on twelve computational cells (Fig. 4a, b) and solution stability is limited by a Courant number equal to unity. If this value is overcome, some spurious oscillations in solution exist (Fig. 4c) leading to expected instability. After space accuracy improvement to second-order, the scheme is more dispersive. This choice makes the stability limit more restrictive. Now, for Cr $\geq$ 0.8 spurious oscillations can be observed (Fig. 4e), however, the wave front is sharper – reproduced on 4 cells (Fig. 4d, e).

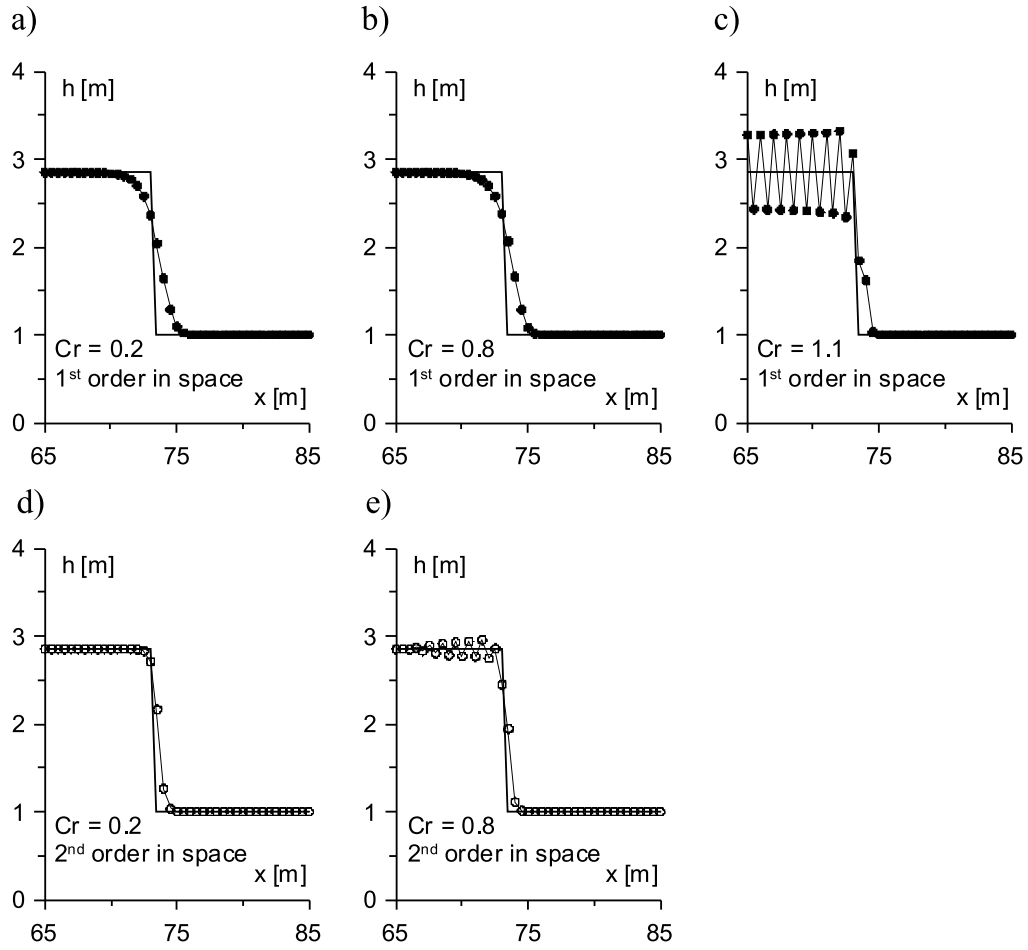

Fig. 4. Front of shock wave after 10 s of simulation – comparison between exact solution (solid lines) and computed using two-step explicit scheme for various space accuracy and Courant numbers (symbols)

Next, the simulations were run using implicit schemes of first-order (Fig. 5a–f) and second-order (Fig. 6a–f) accuracy in time. If the fully implicit ($\Theta = 1$) of first-order accuracy in space is used (Fig. 5a–c), the strong influence of numerical diffusion can be observed, but the wave front location is correctly predicted. This error, occurring due to dissipative properties of this first-order accuracy in both space and time, scheme, is enhanced for increasing Courant numbers and time integration step. If the second-order accuracy in space fully implicit (Euler) scheme is implemented – which is still of first-order accuracy in time – except for numerical diffusion, the incorrect bore position is observed (Fig. 5d–f). Moreover, the depth profile upstream from the wave front is overestimated.

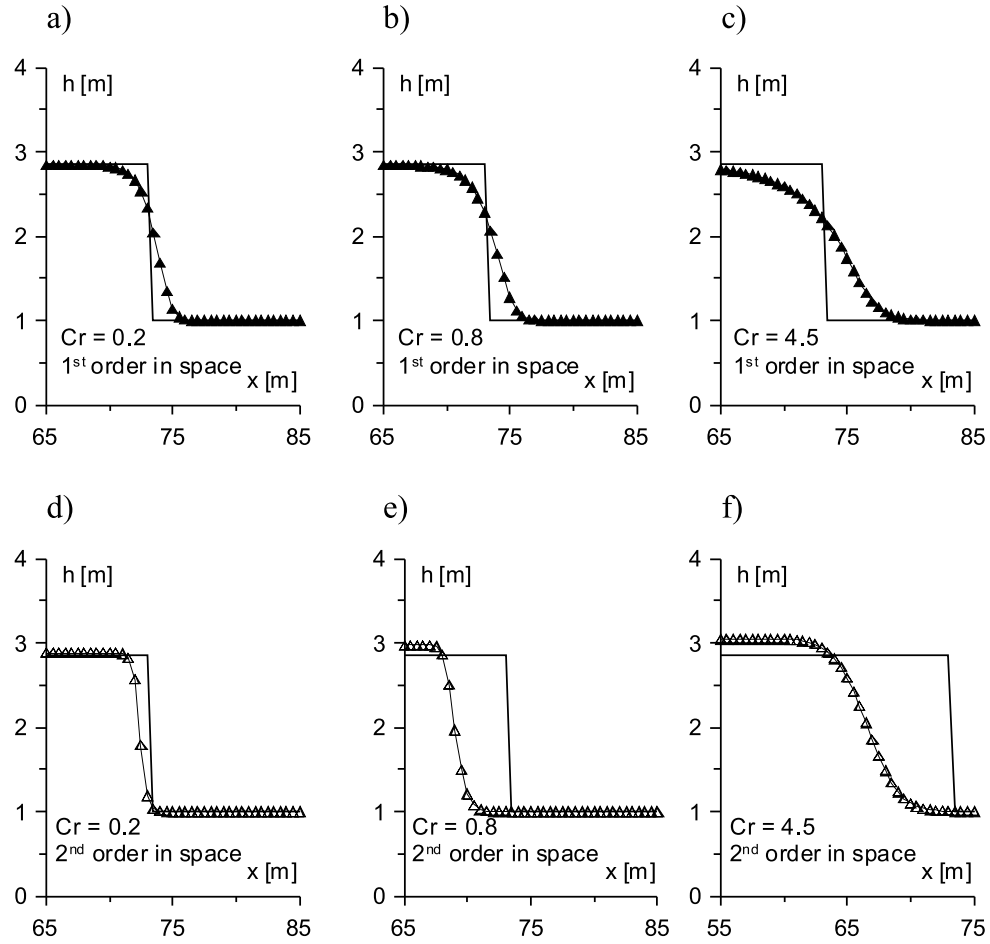

Fig. 5. Front of shock wave after 10 s of simulation – comparison between exact solution (solid lines) and computed using fully implicit scheme (Θ=1) for various space accuracy and Courant numbers (symbols)

In Figures from 6a to 6f the results obtained using implicit trapezoidal scheme ($\Theta = 0.5$) are presented. This one-step implicit scheme is of second-order accuracy in time. Again, if the scheme of first-order accuracy in space is used, the numerical diffusion effect can be observed (Fig. 6a, b). The solution is similar to numerical results obtained using other schemes presented before for a Courant number less than unity. Unfortunately, for Cr $>$ 1 smooth oscillation near front exists, which distorts the shape of wave front (Fig. 6c). Such error is a consequence of numerical dispersion, which is characteristic of the implicit trapezoidal scheme. The influence of dispersive features of that scheme is clearly seen in Figures 6d–f. Now, the scheme is of second-order accuracy in both time and space. The

spurious oscillations are stronger – leading to instability – and the location of front is incorrect.

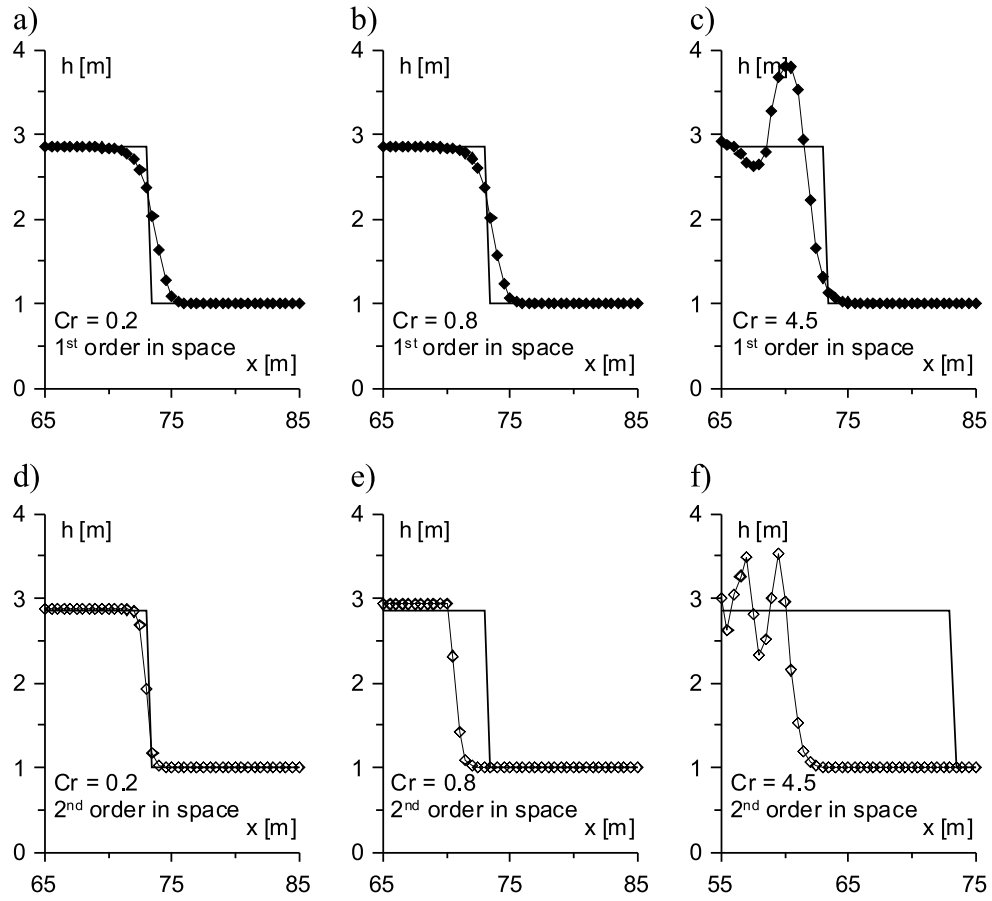

Fig. 6. Front of shock wave after 10 s of simulation – comparison between exact solution (solid lines) and computed using implicit trapezoidal scheme (Θ=0.5) for various space accuracy and Courant numbers (symbols)

Analysing the presented results, it can be seen that all FVM Roe schemes produced sufficiently accurate solution for Cr $<$ 1 and first-order accuracy in space. In such cases there are no oscillations in depth (and velocity) profile and the wave front is predicted correctly. The better shock wave resolution can be ensured if schemes of second-order accuracy in space are implemented. However, such approach requires integration of de Saint-Venant equations with small Courant number, as well as for explicit and implicit schemes. For Cr $>$ 1 the implicit FVM Roe schemes are too dissipative ($\Theta = 1$) or too dispersive ($\Theta = 0.5$).

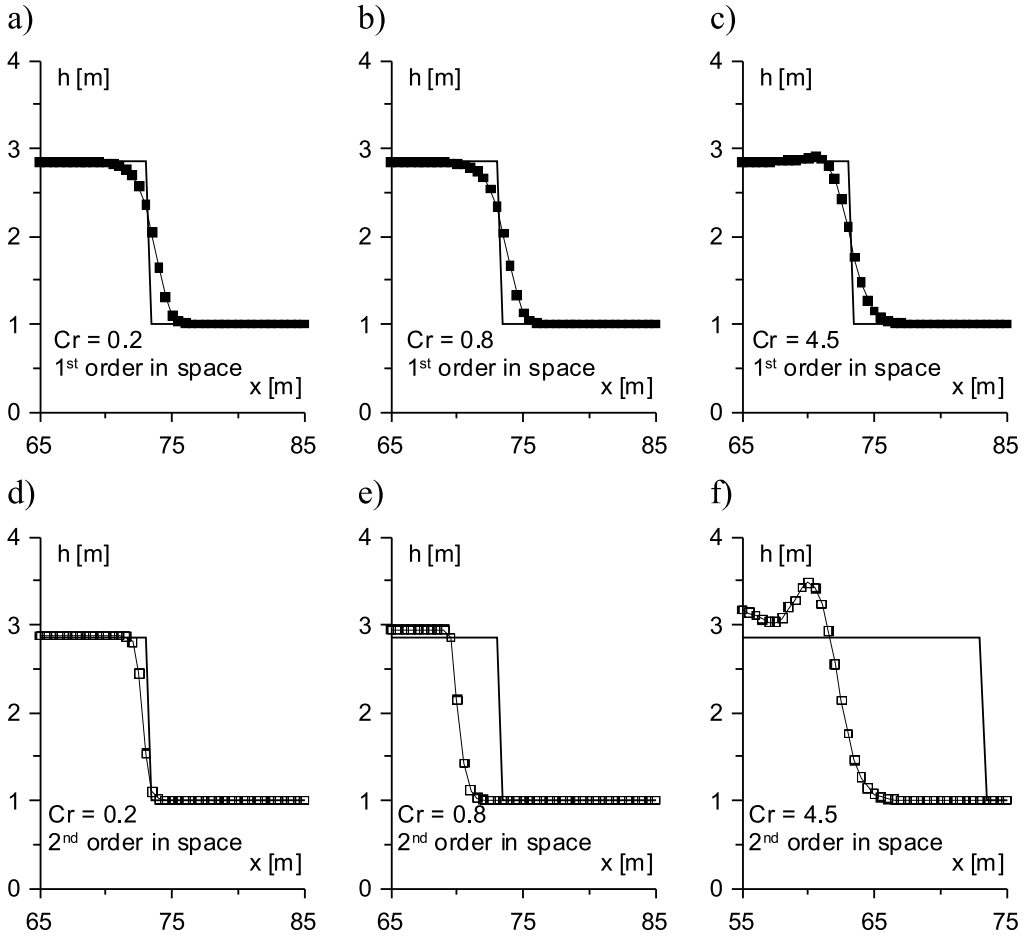

Fig. 7. Front of shock wave after 10 s of simulation – comparison between exact solution (solid lines) and computed using modified implicit scheme (Θ=0.67) for various space accuracy and Courant numbers (symbols)

Investigating the numerical properties of presented FVM schemes similarity to other one step implicit schemes can be observed. The influence of numerical errors on solution accuracy can be compared to the features of the FDM box scheme (Cunge et al 1980) for example. In order to obtain smooth, but not too diffusive numerical solution to de Saint-Venant equations using a box scheme, parameter Θ equal to 0.67 should be applied (Szymkiewicz 2000). The results of implementation of the FVM Roe implicit scheme with $\Theta = 0.67$ for simulation of an idealized dam-break problem are presented in Figures 7a–f. Satisfactory results are obtained if the scheme of first-order accuracy in space (without MUSCL reconstruction) is used (Fig. 7a–c). The numerical solution is devoid of spurious oscillations and even for $Cr > 1$ the numerical diffusion error does not distort the wave front

stronger than for smaller values of Courant number. This important property allows integration of the model equations with larger time step, keeping sufficiently good results' quality. The scheme improvement to second-order accuracy in space once again makes the scheme too dispersive (Fig. 7d–f).

6. Conclusions

Several FVM Roe schemes for modelling one-dimensional, extreme flow with discontinuities, were examined. The numerical simulations were carried out using explicit and implicit time integration technique for different values of Courant number. The results for each scheme were compared with each other and Stoker analytical solution.

It can be concluded that all analysed FVM schemes of first-order accuracy in space, produce similar, reasonable results for a Courant number less than unity. The improvement of accuracy to second-order through application of MUSCL method of function reconstruction, makes the wave fronts resolution better. However, due to numerical dispersion, solution oscillations and incorrect shock position can occur.

For a Courant number greater than one, the explicit scheme becomes – in accordance with expectations – unstable. The solutions obtained using fully implicit and trapezoidal schemes are strongly distorted near the front due to numerical diffusion and dispersion, respectively. The numerical properties of the FVM Roe scheme implicit in time can be improved through parameter Θ modification. Although such a scheme is dissipative, the numerical diffusion does not deform the shape of shock wave front more than other FVM schemes for $Cr < 1$. Moreover, the solution is devoid of oscillations near the front, ensuring smooth profile of water depth even for $Cr > 1$. This is advantageous for flow simulation when a large computational time step is required.

Summing up, the two-step explicit FVM Roe scheme can be recommended for modelling the extreme, rapidly varied flow with discontinuities, when the second-order accuracy both in space and time is indispensable. If the substantial reduction of simulation time is needed, the implicit scheme of first-order accuracy in space with $\Theta = 0.67$ can be successfully applied. The possibility of exceeding the Courant number limitation can be very useful for modelling two-dimensional shallow flows, where large numbers of computational cells are used, and for long time simulations. Additionally, except for well-known, good properties of FVM schemes – like discontinuity handling or good mass conservation – the examined implicit scheme with $\Theta = 0.67$ can be relatively easy extrapolated ensuring solution to de Saint-Venant equations in a channel network. All scheme features mentioned also make it a good candidate for modelling unsteady, rapidly varied flow in storm sewer systems, where subcritical and supercritical, as well as free-surface and pressure flow with numerous transients can be observed.

References

Abbott M. B. (1979), *Computational Hydraulics: Elements of the Theory of Free-Surface Flows*, Pitman, London.

Alcrudo F., Garcia-Navarro P. and Priestley A. (1994), An Implicit Method for Water Flow Modelling in Channels and Pipes, *Journal of Hydraulic Research*, Vol. 32, No. 5, 721–742.

Ambrosi D. (1995), Approximation of Shallow Water Equations by Roe's Riemann Solver, *Int. Journal for Numerical Methods in Fluids*, Vol. 20, 157–168.

Bermudez A. and Vazquez M. E. (1994), Upwind Methods for Hyperbolic Conservation Laws with Source Terms, *Computers and Fluids*, 23, 1049–1071.

Coulson C. A. and Jeffrey A. (1982), *Waves – Mathematical Models* (in Polish), WNT, Warsaw.

Cunge J. A., Holly Jr F. M. and Verwey A. (1980), *Practical Aspects of Computational River Hydraulics*, Pitman, London.

Delis A. I., Skeels C. P. and Ryrie S. C. (2000a), Evaluation of Some Approximate Riemann Solvers for Transient Open Channel Flows, *Journal of Hydraulic Research*, Vol. 38, No. 3, 217–231.

Delis A. I., Skeels C. P. and Ryrie S. C. (2000b), Implicit High-Resolution Methods for Modelling One-Dimesional Open Channel Flow, *Journal of Hydraulic Research*, Vol. 38, No. 5, 369–382.

Glaister P. (1993), Flux Difference Splitting for Open-Channel Flows, *International Journal for Numerical Methods in Fluids*, Vol. 16, 629–654.

Godunov S. K. (1959), A Difference Scheme for Numerical Computation of Discontinuous Solution of Hydrodynamic Equations, *Math. Sbornik*, 47, 271–306.

Goutal N. and Maurel F. (2002), A Finite Volume Solver for 1D Shallow-Water Equations Applied to an Actual River, *Int. Journal for Numerical Methods in Fluids*, Vol. 38, 1–19.

Nujic M. (1995), Efficient Implementation of Non-Oscillatory Schemes for the Computation of Free-Surface Flows, *Journal of Hydraulic Research*, Vol. 3, No. 1.

Potter D. (1977), *Computational Physics* (in Polish), PWN, Warsaw.

Roe P. L. (1981), Approximate Riemann Solvers, Parameters Vectors and Difference Schemes, *Journal of Computational Physics*, 43, 357–372.

Stoker J. J. (1957), *Water Waves*, Interscience Publishers, Wiley, New York.

Szydłowski M. (2001), Two-Dimensional Shallow Water Model for Rapidly and Gradually Varied Flow, *Archives of Hydro-Engineering and Environmental Mechanics*, Vol. 48, No. 1, 35–61.

Szymkiewicz R. (2000), *Mathematical Modelling of Open Channel Flows* (in Polish), PWN, Warsaw.

Tan W. (1992), *Shallow Water Hydrodynamics*, Elsevier, Amsterdam.

Toro E. F. (1997), *Riemann Solvers and Numerical Methods for Fluid Dynamics*, Springer-Verlag, Berlin.

Van Leer B. (1979), Towards the Ultimate Conservative Difference Scheme v.a. Second-Order Sequel to Godunov's Method, *Journal of Computational Physics*, Vol. 32, 101–136.

Zoppou C. and Roberts S. (2003), Explicit Schemes for Dam-Break Simulations, *Journal of Hydraulic Engineering*, Vol. 129, No. 1, 11–34.